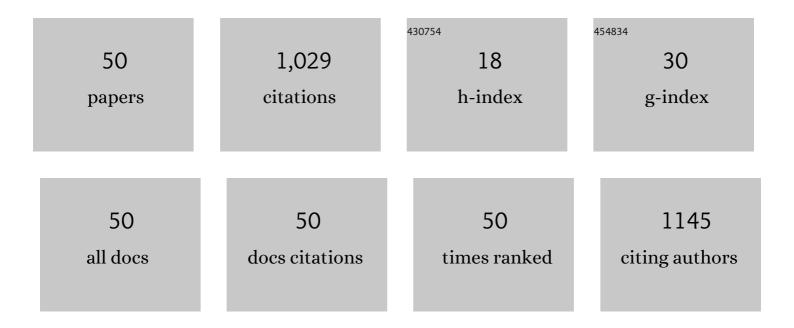
## Yong-Tao Li

List of Publications by Year in descending order

Source: https://exaly.com/author-pdf/8016606/publications.pdf Version: 2024-02-01



#	Article	lF	CITATIONS
1	<scp>Anionâ€Regulated Weakly Solvating</scp> Electrolytes for <scp>Highâ€Voltage</scp> Lithium Metal Batteries. Energy and Environmental Materials, 2023, 6, .	7.3	17
2	Enhancing hydrogen sorption in MgH2 by controlling particle size and contact of Ni catalysts. Rare Metals, 2021, 40, 995-1002.	3.6	43
3	A systematic computational investigation of the water splitting and N <sub>2</sub> reduction reaction performances of monolayer MBenes. Physical Chemistry Chemical Physics, 2021, 23, 6613-6622.	1.3	9
4	Interface controlled solid-state lithium storage performance in free-standing bismuth nanosheets. Dalton Transactions, 2021, 50, 252-261.	1.6	8
5	Enhancement of the ionic conductivity of lithium borohydride by silica supports. Dalton Transactions, 2021, 50, 15352-15358.	1.6	5
6	Fabrication of GeS-graphene composites for electrode materials in lithium-ion batteries. Materials Research Express, 2021, 8, 115013.	0.8	5
7	Effect of cold work on martensitic transformation of Ni38Ti37V25 alloy reinforced by V nanowires. Journal of Alloys and Compounds, 2020, 815, 152489.	2.8	7
8	Reversible room temperature hydrogen storage in high-entropy alloy TiZrCrMnFeNi. Scripta Materialia, 2020, 178, 387-390.	2.6	132
9	Mechanical Synthesis and Hydrogen Storage Characterization of MgVCr and MgVTiCrFe Highâ€Entropy Alloy. Advanced Engineering Materials, 2020, 22, 1901079.	1.6	54
10	The transformation characteristics of the NiTi–V composite with dual-scale bcc-V fibers. Intermetallics, 2020, 116, 106650.	1.8	3
11	Ultra-Fine CeO <sub>2</sub> Particles Triggered Strong Interaction with LaFeO <sub>3</sub> Framework for Total and Preferential CO Oxidation. ACS Applied Materials & Interfaces, 2020, 12, 42274-42284.	4.0	24
12	Crystallite growth characteristics of Mg during hydrogen desorption of MgH2. Progress in Natural Science: Materials International, 2020, 30, 246-250.	1.8	17
13	Boosting Photovoltaic Performance and Stability of Super-Halogen-Substituted Perovskite Solar Cells by Simultaneous Methylammonium Immobilization and Vacancy Compensation. ACS Applied Materials & Interfaces, 2020, 12, 8249-8259.	4.0	19
14	Effects of morphology of V nanowires on superelasticity of Ti46Ni44V10 alloy. Materials Science & Engineering A: Structural Materials: Properties, Microstructure and Processing, 2020, 786, 139450.	2.6	2
15	In situ forming LiF nanodecorated electrolyte/electrode interfaces for stable all-solid-state batteries. Materials Today Nano, 2020, 10, 100079.	2.3	38
16	Enhanced Low-Temperature Hydrogen Storage in Nanoporous Ni-Based Alloy Supported LiBH4. Frontiers in Chemistry, 2020, 8, 283.	1.8	10
17	Turning bulk materials into 0D, 1D and 2D metallic nanomaterials by selective aqueous corrosion. Chemical Communications, 2019, 55, 10476-10479.	2.2	12
18	Potassium octahydridotriborate: diverse polymorphism in a potential hydrogen storage material and potassium ion conductor. Dalton Transactions, 2019, 48, 8872-8881.	1.6	34

Yong-Tao Li

#	Article	IF	CITATIONS
19	Enhanced hydrogen storage kinetics of an Mg–Pr–Al composite by in situ formed Pr3Al11 nanoparticles. Dalton Transactions, 2019, 48, 7735-7742.	1.6	15
20	Effect of Microstructure on Hydrogen Permeation in EA4T and 30CrNiMoV12 Railway Axle Steels. Metals, 2019, 9, 164.	1.0	4
21	Controlled phase evolution from Cu <sub>0.33</sub> Co <sub>0.67</sub> S <sub>2</sub> to Cu <sub>3</sub> Co <sub>6</sub> S <sub>8</sub> hexagonal nanosheets as oxygen evolution reaction catalysts. RSC Advances, 2019, 9, 9729-9736.	1.7	11
22	Uniform gallium oxyhydroxide nanorod anodes with superior lithium-ion storage. RSC Advances, 2019, 9, 34896-34901.	1.7	7
23	Hydrogen Storage Properties and Reactive Mechanism of LiBH4/Mg10YNi-H Composite. Materials Research, 2019, 22, .	0.6	1
24	Carbon/Sulfur Composites Stabilized with Nano-TiNi for High-Performance Li–S Battery Cathodes. ACS Applied Energy Materials, 2019, 2, 1537-1543.	2.5	9
25	Activity-Tuning of Supported Co–Ni Nanocatalysts via Composition and Morphology for Hydrogen Storage in MgH2. Frontiers in Chemistry, 2019, 7, 937.	1.8	17
26	Improving the phase stability and cycling performance of Ce <sub>2</sub> Ni <sub>7</sub> -type RE–Mg–Ni alloy electrodes by high electronegativity element substitution. Dalton Transactions, 2018, 47, 16453-16460.	1.6	19
27	Thermal Dehydrogenation Characteristics of Li-Sr-Al-N-H Hydrogen Storage System. Materials Research, 2018, 21, .	0.6	0
28	Transformation and superelastic characteristics of large hysteresis TiNi matrix shape memory alloys reinforced by V nanowires. Materials Letters, 2018, 228, 391-394.	1.3	14
29	Effect of plastic deformation of V nanowires on the transformation characteristics of NiTiV alloys. Materials Science & Engineering A: Structural Materials: Properties, Microstructure and Processing, 2018, 735, 162-165.	2.6	11
30	Intrinsic alterations in the hydrogen desorption of Mg <sub>2</sub> NiH <sub>4</sub> by solid dissolution of titanium. Dalton Transactions, 2018, 47, 8418-8426.	1.6	11
31	Solid solution of Cu in Mg2NiH4 and its destabilized effect on hydrogen desorption. Materials Chemistry and Physics, 2017, 193, 1-6.	2.0	19
32	Hydrogen-induced magnesium–zirconium interfacial coupling: enabling fast hydrogen sorption at lower temperatures. Journal of Materials Chemistry A, 2017, 5, 5067-5076.	5.2	94
33	The superior desorption properties of MgCl <sub>2</sub> -added ammonia borane compared to MgF <sub>2</sub> -added systems—the unexpected role of MgCl <sub>2</sub> interacting with [NH <sub>3</sub> ] units. RSC Advances, 2017, 7, 36684-36687.	1.7	3
34	Self-Printing on Graphitic Nanosheets with Metal Borohydride Nanodots for Hydrogen Storage. Scientific Reports, 2016, 6, 31144.	1.6	20
35	Enhancement of Hydrogen Storage in Destabilized LiNH <sub>2</sub> with KMgH <sub>3</sub> by Quick Conveyance of N-Containing Species. Journal of Physical Chemistry C, 2016, 120, 1415-1420.	1.5	28
36	Direct mechanochemical formation of alkali metal borohydrides nanocrystals exhibiting kinetic and thermodynamic destabilizations. International Journal of Hydrogen Energy, 2016, 41, 2807-2813.	3.8	0

Yong-Tao Li

#	Article	IF	CITATIONS
37	Comparative Investigations on Hydrogen Absorption–Desorption Properties of Sm–Mg–Ni Compounds: The Effect of [SmNi5]/[SmMgNi4] Unit Ratio. Journal of Physical Chemistry C, 2015, 119, 4719-4727.	1.5	33
38	Facile preparation of carbon-coated Mg nanocapsules as light microwave absorber. Materials Letters, 2015, 149, 12-14.	1.3	20
39	Facile self-assembly of light metal borohydrides with controllable nanostructures. RSC Advances, 2014, 4, 983-986.	1.7	19
40	Enhanced reducibility and redox stability of Fe <sub>2</sub> O <sub>3</sub> in the presence of CeO <sub>2</sub> nanoparticles. RSC Advances, 2014, 4, 47191-47199.	1.7	70
41	<i>In Situ</i> Embedding of Mg <sub>2</sub> NiH <sub>4</sub> and YH <sub>3</sub> Nanoparticles into Bimetallic Hydride NaMgH <sub>3</sub> to Inhibit Phase Segregation for Enhanced Hydrogen Storage. Journal of Physical Chemistry C, 2014, 118, 23635-23644.	1.5	33
42	Hydrogen storage of a novel combined system of LiNH <sub>2</sub> –NaMgH <sub>3</sub> : synergistic effects of in situ formed alkali and alkaline-earth metal hydrides. Dalton Transactions, 2013, 42, 1810-1819.	1.6	17
43	Carbon nanomaterial-assisted morphological tuning for thermodynamic and kinetic destabilization in sodium alanates. Journal of Materials Chemistry A, 2013, 1, 5238.	5.2	30
44	Fast hydrogen-induced optical and electrical transitions of Mg and Mg-Ni films with amorphous structure. Applied Physics Letters, 2013, 102, .	1.5	17
45	Promoted hydrogen release from 3LiBH4/MnF2 composite by doping LiNH2: Elimination of diborane release and reduction of decomposition temperature. International Journal of Hydrogen Energy, 2012, 37, 18074-18079.	3.8	4
46	Enhanced dehydrogenation of ammonia borane by reaction with alkaline earth metal chlorides. International Journal of Hydrogen Energy, 2012, 37, 4274-4279.	3.8	20
47	Hydrogen storage properties of TiMn1.5V0.2-based alloys for application to fuel cell system. Journal of Power Sources, 2010, 195, 8215-8221.	4.0	19
48	Improved dehydrogenation of TiF <sub>3</sub> -doped NaAlH <sub>4</sub> using ordered mesoporous SiO <sub>2</sub> as a codopant. Journal of Materials Research, 2010, 25, 2047-2053.	1.2	19
49	Pressure hysteresis in the TiMn <sub>1.5</sub> V <i><sub>x</sub></i> -H <sub>2</sub> ( <i>x</i> = 0.1–0.5) system. Journal of Materials Research, 2009, 24, 2886-2891.	1.2	5
50	Phase component and microstructure of laser-sintered Mg-Ni alloys. Rare Metals, 2008, 27, 400-404.	3.6	1